Title
Liquefaction-Induced Lateral Spreading at Izmit Bay During the Kocaeli (Izmit)-Turkey Earthquake

Journal
Journal of Geotechnical & Geoenvironmental Engineering, 130(12)

Authors
Cetin, K. Onder
Youd, T Leslie
Seed, Raymond B
et al.

Publication Date
2004

Peer reviewed

Liquefaction-Induced Lateral Spreading at Izmit Bay During the Kocaeli (Izmit)-Turkey Earthquake

K. Onder Cetin, M.ASCE[1]; T. Leslie Youd, M.ASCE[2]; Raymond B. Seed, M.ASCE[3]; Jonathan D. Bray, M.ASCE[4]; Jonathan P. Stewart, M.ASCE[5]; H. Turan Durgunoglu, M.ASCE[6]; W. Lettis, M.ASCE[7]; and M. Tolga Yilmaz[8]

Abstract: This paper presents a study of liquefaction-induced lateral ground displacements along the coast of Izmit Bay during the 1999 Kocaeli (Izmit)-Turkey earthquake. The paper discusses: (1) observed ground displacements after the earthquake, (2) the results of field investigations by means of borings and in situ index tests, including standard penetration tests, static cone penetration tests, and piezocone tests, (3) analyses of expected lateral displacements using two empirical models and one semiempirical model, and (4) comparisons between observed and calculated lateral ground movements. The three models provide inconsistent predictions of observed lateral ground displacements, with one method overpredicting and two methods both overpredicting and underpredicting observed lateral ground displacements by large amounts. Thus, it appears that there is a need for improved engineering tools for prediction of small to moderately significant lateral ground displacements (lateral displacements of approximately 0.1–2.5 m) at soil sites with similar ground characteristics to the case history sites presented herein.

DOI: 10.1061/(ASCE)1090-0241(2004)130:12(1300)

CE Database subject headings: Earthquakes; Liquefaction; Lateral displacement; Seismic hazard; Turkey; Bays.

Introduction

The 17 August 1999 Kocaeli-Turkey earthquake was an event of magnitude $M_w=7.4$, and caused extensive liquefaction-induced ground displacements along the coast of Izmit Bay. This paper presents a study of the liquefaction-induced ground displacements observed at a number of sites; the police station, soccer field, Degirmendere nose, and Yalova Harbor sites along the southern coast of Izmit Bay, as shown in Fig. 1. Within this paper's confines, geologic setting and recorded ground motions at the soil sites during the Kocaeli earthquake, the observed liquefaction-induced lateral ground displacements, and the results of site investigations and in situ index tests including standard penetration tests (SPT), static cone penetration tests (CPT), and piezocone (CPTU) tests are discussed. These site investigation results are then used as a basis for calculation, by three analytical procedures, of expected lateral ground displacements. Finally, a comparison is made between the observed ground displacements and the results of these three sets of ground displacement calculations.

Geologic Setting

The Gulf of Izmit is situated in an east–west trending active graben system which is dynamically affected by the interaction of the North Anatolian Fault zone and the Marmara Graben system. It is bounded by two horsts: (1) Kocaeli Peninsula to the north and (2) the Armutlu Peninsula to the south, exhibiting completely different geomorphologic features, and by well defined fault scarps. The graben, varying in the range of 6–10 km in width, is a comparatively large, long and narrow basin filled with young sediments of marine and continental facies (Seymen 1995). As shown in Fig. 2, the southern shores of Izmit Bay are covered by Holocene deposits except a relatively small area, which was classified geologically as Bakacak formation of Companian-Maastrihtien age consisting of marn, mudstone, conglomerate, and sandstone. From a sedimentalogical point of view, the southern shores of Izmit Bay are covered principally by fine-grained sandy deposits which get finer (siltier and more clayey) towards the north into the depths of Izmit Bay.

Ground Motions during 1999 Kocaeli Earthquake

The Kocaeli (Izmit) earthquake occurred in northwestern Turkey at 3:02 a.m. (local time) on August 17, 1999 along a 125 km

[1]Associate Professor, Dept. of Civil Engineering, Middle East Technical Univ., 06531 Ankara, Turkey.

[2]Professor, Dept. of Civil and Environmental Engineering, Brigham Young Univ., Provo, UT 84602.

[3]Professor, Dept. of Civil and Environmental Engineering, Univ. of California at Berkeley, Berkeley, CA 94720.

[4]Professor, Dept. of Civil and Environmental Engineering, Univ. of California at Berkeley, Berkeley, CA 94720.

[5]Associate Professor, Dept. of Civil and Environmental Engineering, Univ. of California, Los Angeles, CA 90095.

[6]Professor, Dept. of Civil Engineering, Bogazici Univ., 80815 Bebek, Istanbul, Turkey.

[7]William Lettis and Associates, Inc., Walnut Creek, CA 94596.

[8]Graduate Student Researcher, Dept. of Civil Engineering, Middle East Technical Univ., 06531 Ankara, Turkey.

Note. Discussion open until May 1, 2005. Separate discussions must be submitted for individual papers. To extend the closing date by one month, a written request must be filed with the ASCE Managing Editor. The manuscript for this paper was submitted for review and possible publication on July 11, 2003; approved on February 16, 2004. This paper is part of the ***Journal of Geotechnical and Geoenvironmental Engineering***, Vol. 130, No. 12, December 1, 2004. ©ASCE, ISSN 1090-0241/2004/12-1300–1313/$18.00.

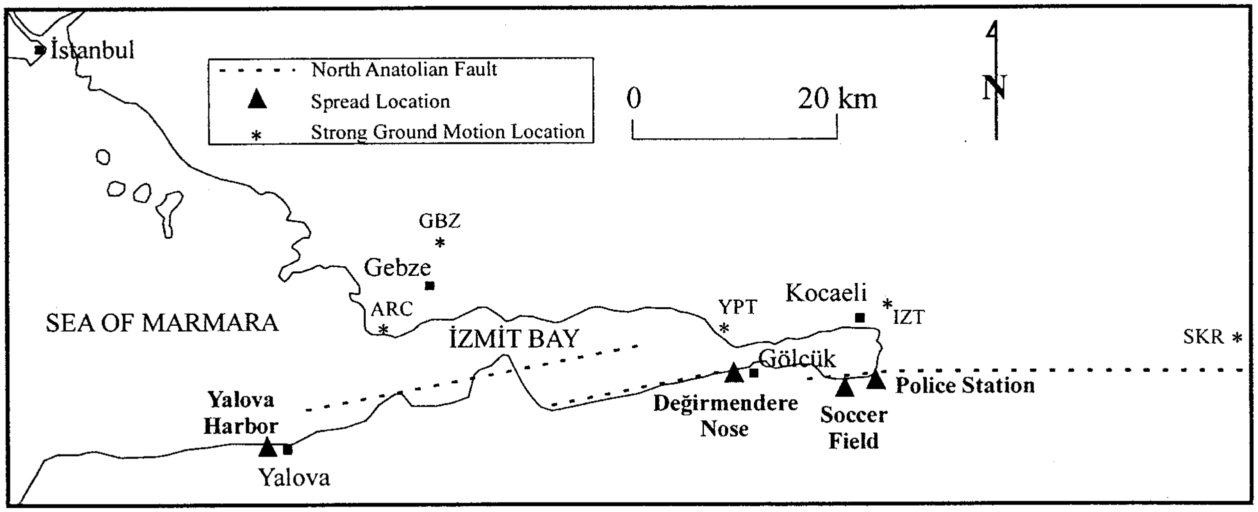

Fig. 1. Case history site map

segment of the North Anatolian Fault, as shown in Fig. 1. The earthquake ($M_w = 7.4$) generated a large number of ground-motion recordings within 20 km of the fault rupture. Table 1 presents a summary of select near fault strong ground-motion stations, and key characteristics of these records. Event-specific attenuation relationships suggest that the peak horizontal ground acceleration on a hypothetical "rock outcrop" and on soft soil at the police station, soccer field, Degirmedere Nose, and Yalova Harbor sites, located within a maximum of 2–3 Km from the fault rupture, would have been about 0.3–0.45g. Most conventional attenuation relationships available prior to the event tend to overpredict the observed near-field levels of shaking. However, if the attenuation relationship proposed by Abrahamson and Silva (1997) is scaled, on an event-specific local basis, using the near-field Izmit, Yarimca and Gebze station recordings, then the soft soil site peak horizontal ground accelerations at about comparable fault distances are estimated approximately as 0.40g for the police station, soccer field, and Degirmedere Nose sites and 0.30g for the Yalova Harbor site. In addition to available strong ground motion records, the results of one-dimensional equivalent linear site response studies performed using *SHAKE-91* (Idriss and Sun 1992) led to the conclusion that the peak horizontal ground acceleration at these soil sites was on the order of 0.30–0.40g. The levels of observed damage to the buildings and their contents at these sites also support this conclusion.

Field Investigations

Field investigations included rotary wash borings and in situ SPTs, CPTs, and CPTUs. A total of 10 SPT borings, 6 CPT, and 9

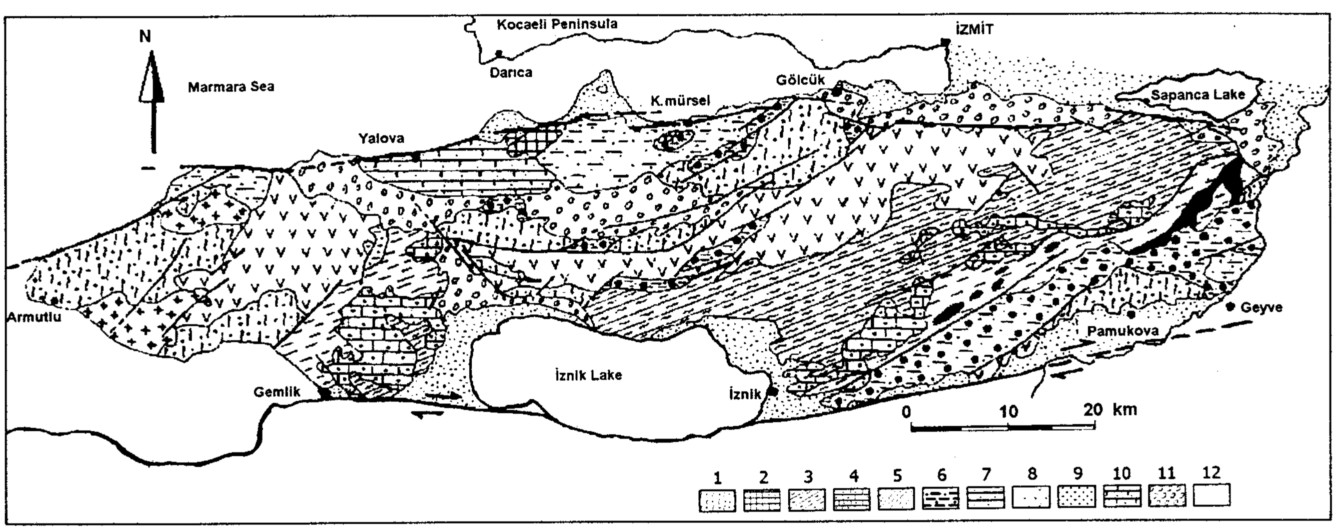

Fig. 2. Simplified geological map of Armutlu peninsula (after Goncuoglu et al. 1992): (1) Pamukova metamorphics, (2) sedimentary cover of Pamukova metamorphics (Triassic) (Ballikaya formation); (3) lower part of the İznik Metamorphics (Triassic); (4) Alicyayla limestone (Upper Triassic–Middle Jurassic); (5) upper part of the Iznik Metamorphics, ophiolitic metaolistostrome: black shading shows ophiolitic rocks (Upper Jurassic–Lower Cretaceous); (6) Bakacak formation (Campanian—Maastrichtian); (7) Incebel formation (Paleocene–Lutetian); (8) Sarisu volcanics (Lutetian); (9) Fistikli granitoid (Eocene); (10) Kilinc formation (Sarmasiyan/Ponsian); (11) Pliocene detritals; and (12) recent deposits

Table 1. Summary of Selected Main Shock Strong Motion Records (after Safak et al. 2000), Locations of Recording Stations Are Shown in Fig. 1.

Station	Station coordinates	Distance to rupture plane (km)	Site class	Peak horizontal acceleration (g)	
				Strong composition	Weak composition
Arcelik (ARC)	40.830° N 29.360° E	17	Stiff Soil	0.211 (W)	0.134 (S)
Gebze (GBZ)	40.820° N 29.440° E	17	Stiff Soil	0.144 (W)	0.266 (N)
Yarimca (YPT)	40.763° N 29.761° E	4.4	Soft Soil	0.262 (E)	0.298 (N)
Izmit (IZT)	40.790° N 29.960° E	7.7	Rock	0.226 (E)	0.169 (S)
Sakarya (SKR)	40.737° N 30.384° E	3.3	Stiff Soil	0.407 (E)	N/A (S)

CPTU soundings were performed at these sites. Standard penetration tests were performed in close conformance with the guidelines recommended by Seed et al. (1985), with direct driving energy measurements taken on some of the SPT tests. Cone penetration test and CPTUs were performed in conformance with *D6066-98* standards (ASTM 2000). A detailed presentation of individual boring logs and other in situ test results will be discussed next, and is also available at ⟨http://peer.berkeley.edu/turkey/adapazari⟩.

Ground Displacement Surveys

Due to possible caving of the fissure faces or simply stretching of the fissures, estimating lateral ground displacements from open ground fissures can be erroneous unless careful attention is given to match pre-earthquake contact points across the fissure. Remembering this fact, "undisturbed" ground fissures were carefully mapped to eliminate possible stretching or caving problems by one or more of the authors of this paper within 1–3 weeks after the earthquake. Postearthquake topographical studies were also performed in the following days to verify and support these ground displacement maps.

Police Station Site

Site Description and Subsurface Soil Conditions

The police station site is located on the east shore of Izmit Bay, in the town of Golcuk, as shown in Fig. 1. Lateral spreading ground displacements were observed behind 2-story structures located approximately 100 m inboard from the shoreline. The near shoreline is only 15 m from the surface fault rupture where it exits from Izmit Bay.

Soil conditions across the site are represented by three interpreted cross sections, as shown in Figs. 3–6. These cross sections are largely perpendicular to the shoreline and/or parallel to the principal direction of lateral ground displacements. In general, the subsurface soil conditions at these cross sections are laterally relatively consistent. Surfacial soils consist of artificial fill comprised of poorly graded gravelly sand, ranging in thickness from 1.5 to 2.0 m. This fill layer is underlain by a 1.5–2.0 m thick loose gray silty sand layer. Energy corrected SPT blow counts $(N)_{60}$ are as low as 3 blows/ft in this silty sand layer. At about 4 m depth, a soft and low plasticity silty clay layer about 3.5–4 m in thickness is present. Liquid limits (LLs) and plasticity indices (PIs) of the layer are 40–45 and 18–23, respectively. This silty clay layer is underlain by a 1.5 m thick very loose to loose silty sand layer. Below this layer there lies a soft and low plasticity silty clay layer with LL and PI values of 37 and 17, respectively.

Observed Liquefaction-Induced Lateral Ground Displacements

At the police station site, mapped ground cracks due to lateral spreading were as wide as 0.64 m (Fig. 3). Ground displacements continued to accrue with increased proximity to the shoreline, and lateral ground displacements reach to a total of about 2.4 m at the shore of Izmit Bay along cross sections I, II, and III in Figs. 3–6. Localized mapping of ground displacements was facilitated by both ground surveys, as well as by mapping and measurement of offsets across ground fissures throughout the site.

Soccer Field Site

Site Description and Subsurface Soil Conditions

Lateral spreading ground displacements were observed at a soccer field located on the south–east shore of Izmit Bay, approximately 8.5 km east of town of Golcuk, as shown in Fig. 1.

Subsurface soil conditions across the site are represented by two interpreted cross sections as shown in Figs. 7–9. These two cross sections are largely perpendicular to the shoreline and/or parallel to the principal direction of lateral ground displacements. In general, the subsurface soil conditions at these cross sections are laterally relatively consistent. Surfacial soils consist of artificial fill comprised of brown silty clay, ranging in thickness from 0.5 to1.5 m. This fill layer is underlain by a 2.0–2.5 m thick silty sand and silt layers. Energy corrected SPT blow counts $(N)_{60}$ are on the order of 3 blows/ft in this silty sand layer. At about 3.5 m depth, a soft high plasticity silty clay layer is present. The values for LL and PI of the layer are in the range of 50–60, and 30–35, respectively.

Observed Liquefaction-Induced Lateral Ground Displacements

As shown in Fig. 7, at the soccer field site ground displacements accrue with increased proximity to the shoreline, and lateral ground displacements reached a total of about 1.2 m at the shore of Izmit Bay along cross sections I and II, in Figs. 8 and 9.

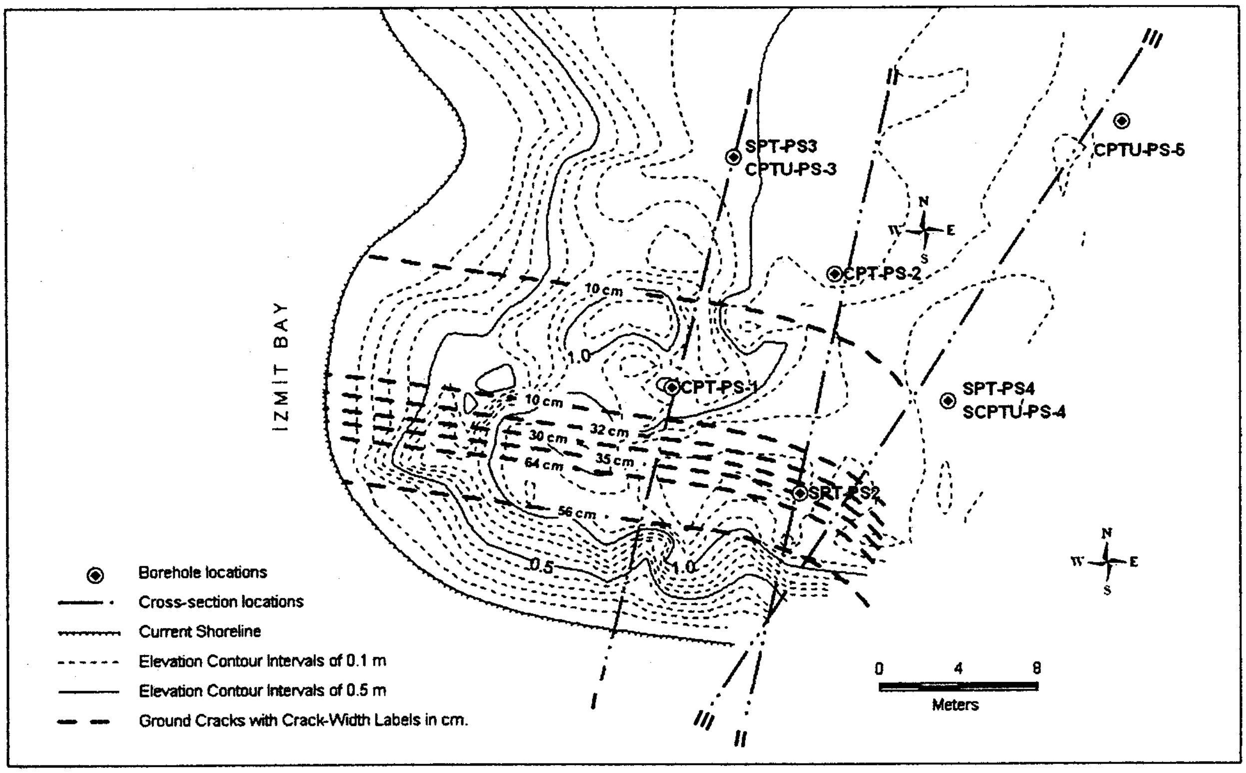

Fig. 3. Ground displacement map of police station site

Localized mapping of ground displacements was facilitated by ground surveys. At about 70 m inboard from the shoreline, signs of ground displacements in the form of lateral spreading disappear.

Degirmendere Nose

Site Description and Subsurface Soil Conditions

As is evident from the name of the site, the Degirmendere Nose site is located at the north edge of the town of Degirmendere, on a small peninsular intrusion into the Bay of Izmit as shown in Fig. 10. At Degirmendere Nose, there existed a municipality owned hotel and recreational area. During the earthquake, following slumping of the fill material, the site was inundated. All of the recreational facilities, as well as the municipality hotel, were lost into the Marmara Sea, along with its residents. The failure mechanism was attributed to fault induced slope instability and/or liquefaction of underlying fill materials (Cetin et al. 2004). The ground surface slopes towards the bay at an average angle of approximately 10–15°.

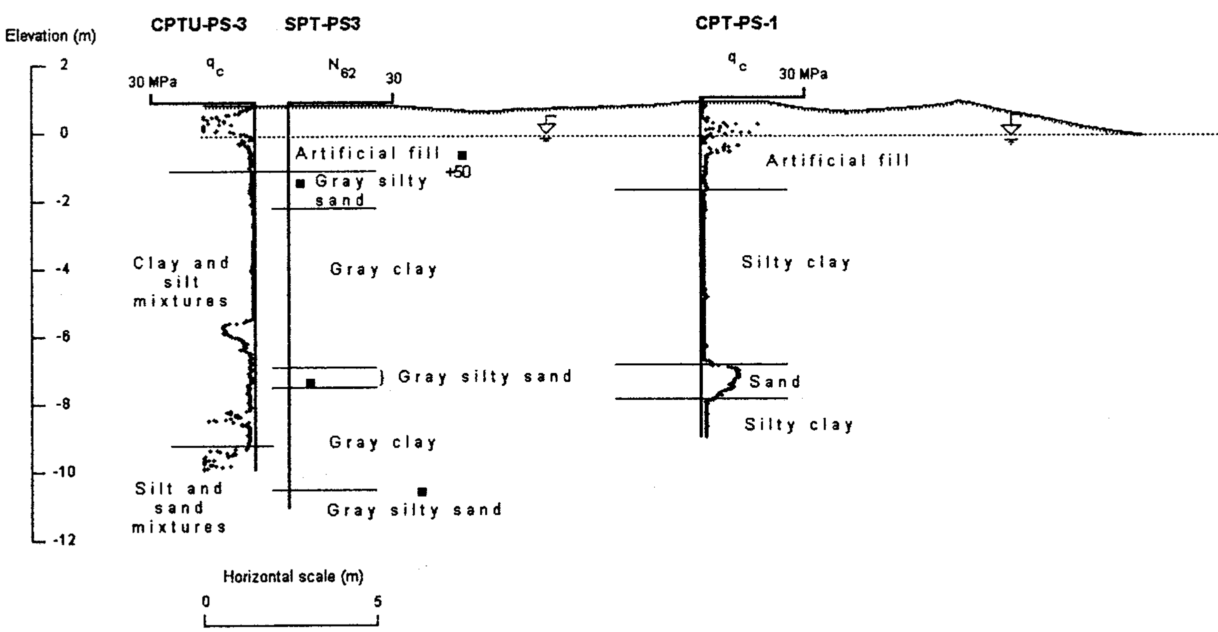

Fig. 4. Cross section I-I of police station site

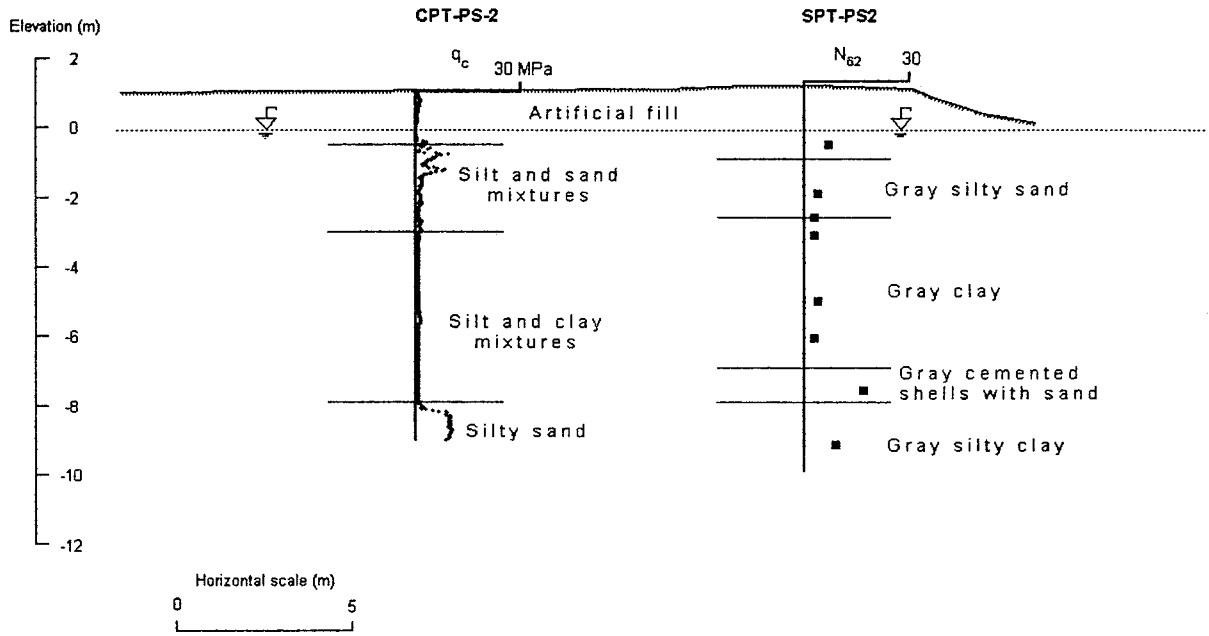

Fig. 5. Cross section II-II of police station site

Soil conditions across the site are represented by one interpreted cross section largely perpendicular to the shoreline and parallel to the direction of lateral ground displacements as shown in Fig. 11. Surfacial soils consist of artificial fill comprised of brown gravelly sand to red silty clay ranging in thickness from 0.5 to 1 m. This fill layer is underlain by a thick silty sand layer with occasional gravelly sand and silty clay mixtures. Energy corrected SPT blow counts $(N)_{60}$ are in the range of 15–20 blows/ft in this silty sand layer. The fines content of the material is generally in the range of 10–30%.

Observed Liquefaction-Induced Lateral Ground Displacements

At the Degirmendere Nose site, three major lines of ground cracks were surveyed parallel to the shoreline, located between the park area and the residential buildings to the east. The crack widths were measured approximately as 9, 50, and 28 cm, respectively, summing to a total of 87 cm along the survey section perpendicular to the shoreline. The orientation as well as the location of the crack lines relative to the shoreline is presented in Fig. 10.

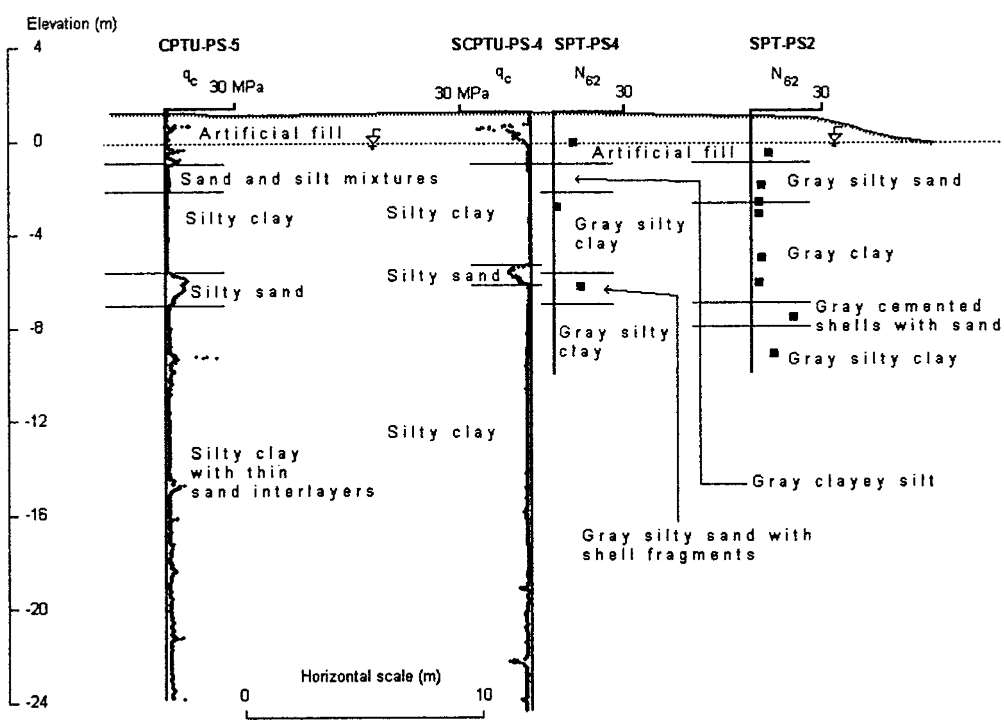

Fig. 6. Cross section III-III of police station site

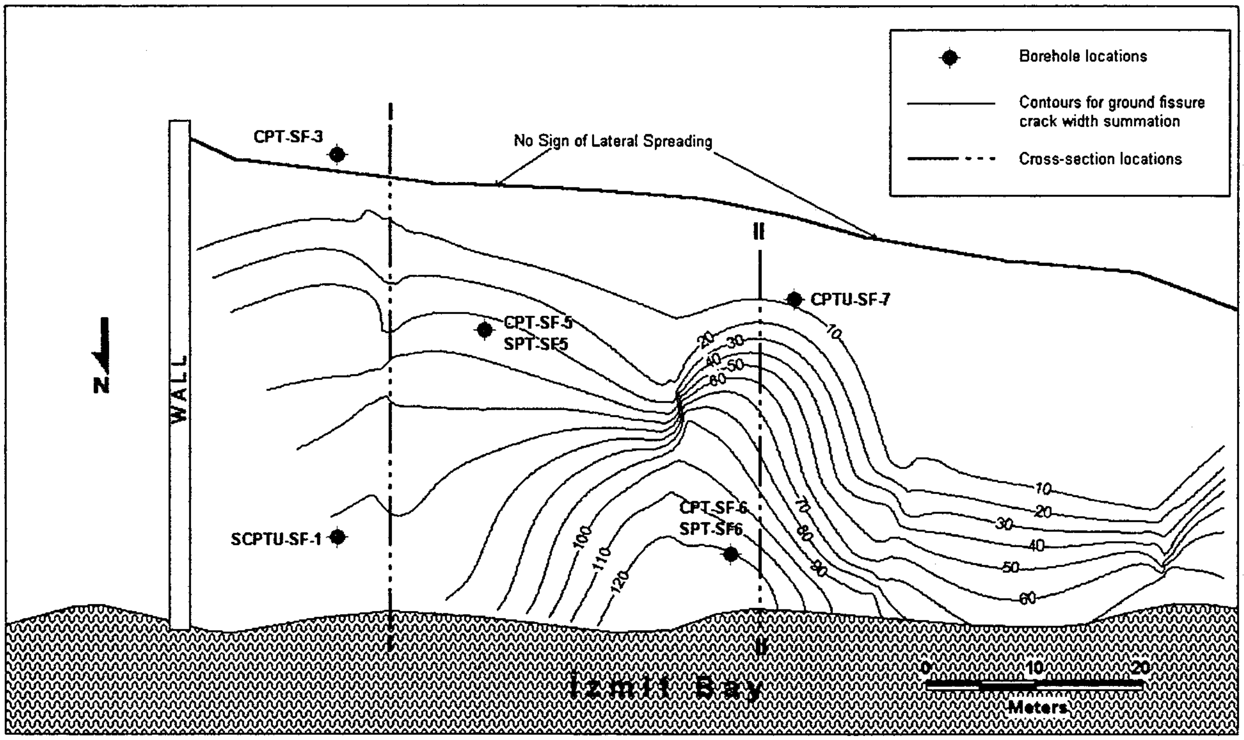

Fig. 7. Ground displacement map of soccer field site

At about 50 m inboard from the shoreline, signs of ground displacements in the form of lateral spreading disappear.

Yalova Harbor

Site Description and Subsurface Soil Conditions

The Yalova Harbor site is located on the western shore of Izmit Bay, approximately 0.5 km west of downtown Yalova, as shown in Fig. 1. Lateral spreading ground displacements were observed at the fishermen's wharf adjacent to the Yalova Ferry Harbor.

Subsurface soil conditions across the site are represented by one interpreted cross section largely parallel to the direction of lateral ground displacements, as shown in Figs. 12 and 13. The surface of the site is covered with cobblestone pavements underlain by artificial fill comprised of gravelly silty sand ranging in thickness from 0.5 to 1 m. This fill layer is underlain by a 7 m thick nonplastic silty sand layer with fines content in the range of

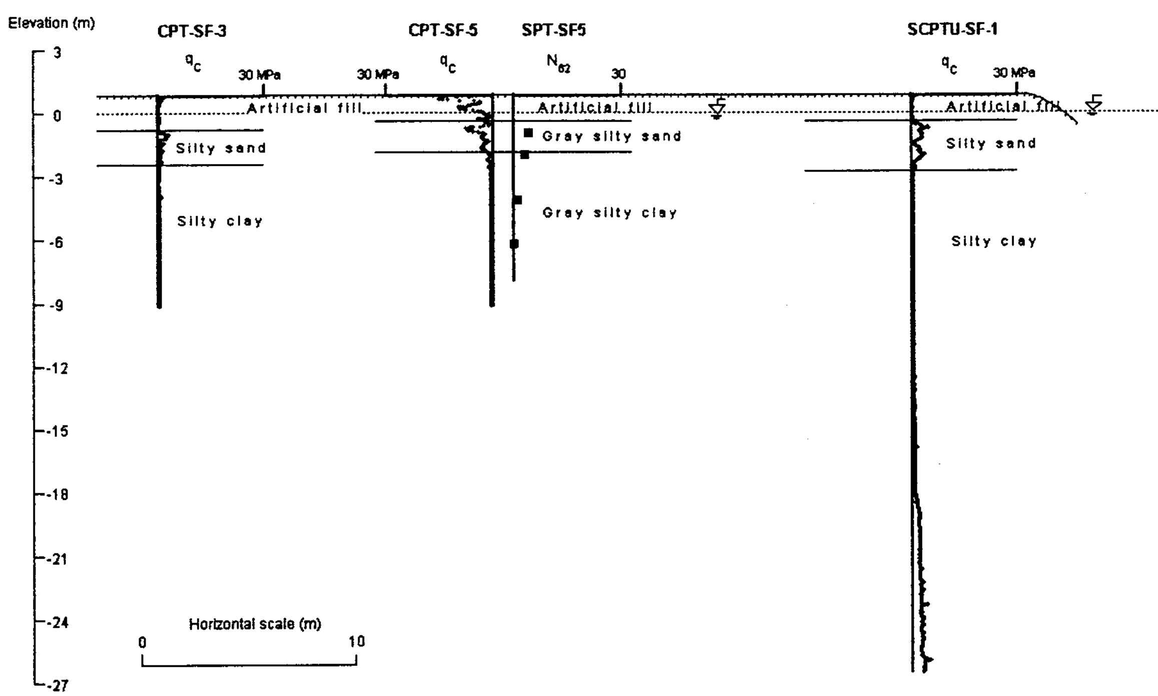

Fig. 8. Cross section I-I of soccer field site

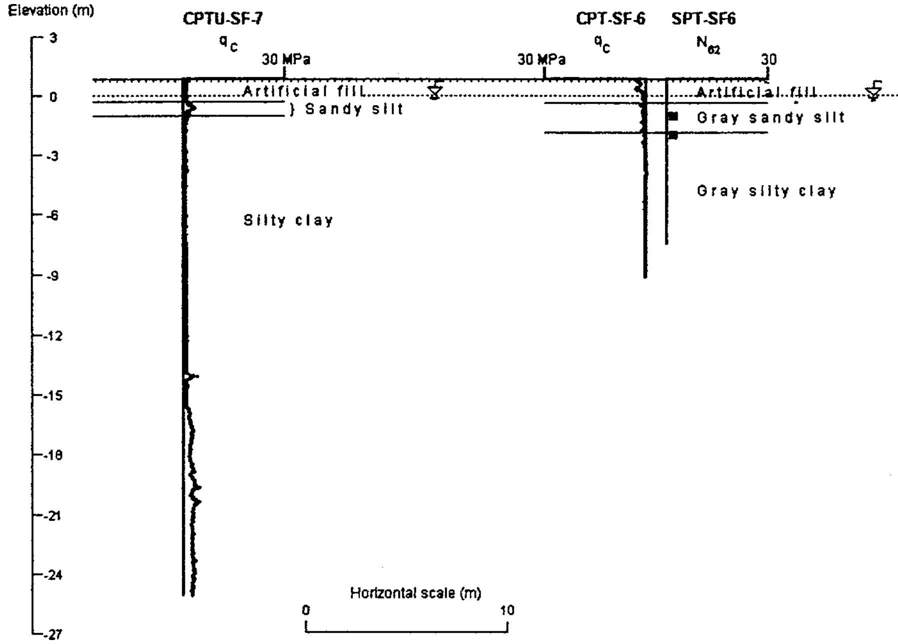

Fig. 9. Cross section II-II of soccer field site

10–35%. Energy corrected SPT blow counts $(N)_{60}$ are 5–10 blows/ft in this silty sand layer. Fines content of the material are 10–30% in this layer. Underlying this silty sand layer is an 8 m thick silty clay to clayey silt layer of low plasticity. Liquid limit and PI of the layer are 30–45, and 20–25, respectively. The plasticity of the clay layer increases with depth within the layer. A silty sand layer of unknown thickness underlies this layer.

Observed Liquefaction-Induced Lateral Ground Displacements

As shown in Fig. 12, at the Yalova Harbor Site, ground displacements accrue with increased proximity to the shoreline, and lateral ground displacements increase in the northwest directions

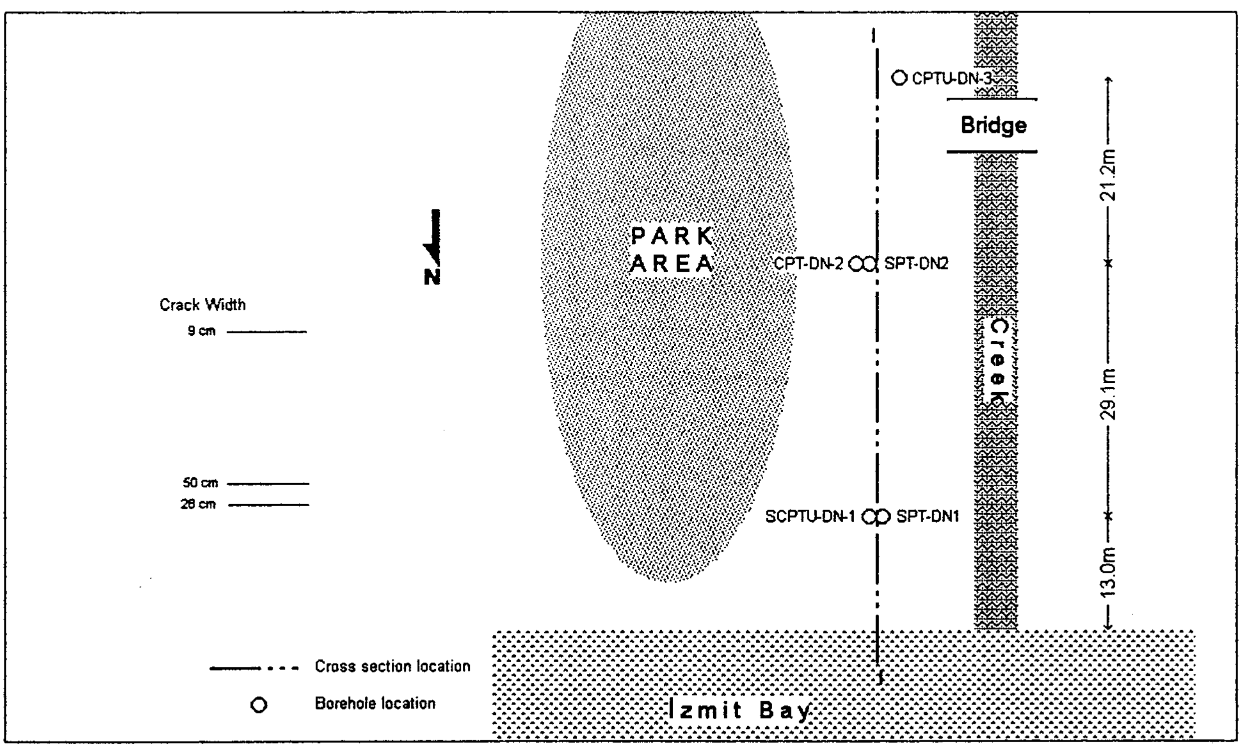

Fig. 10. Ground displacement map of Degirmendere Nose site

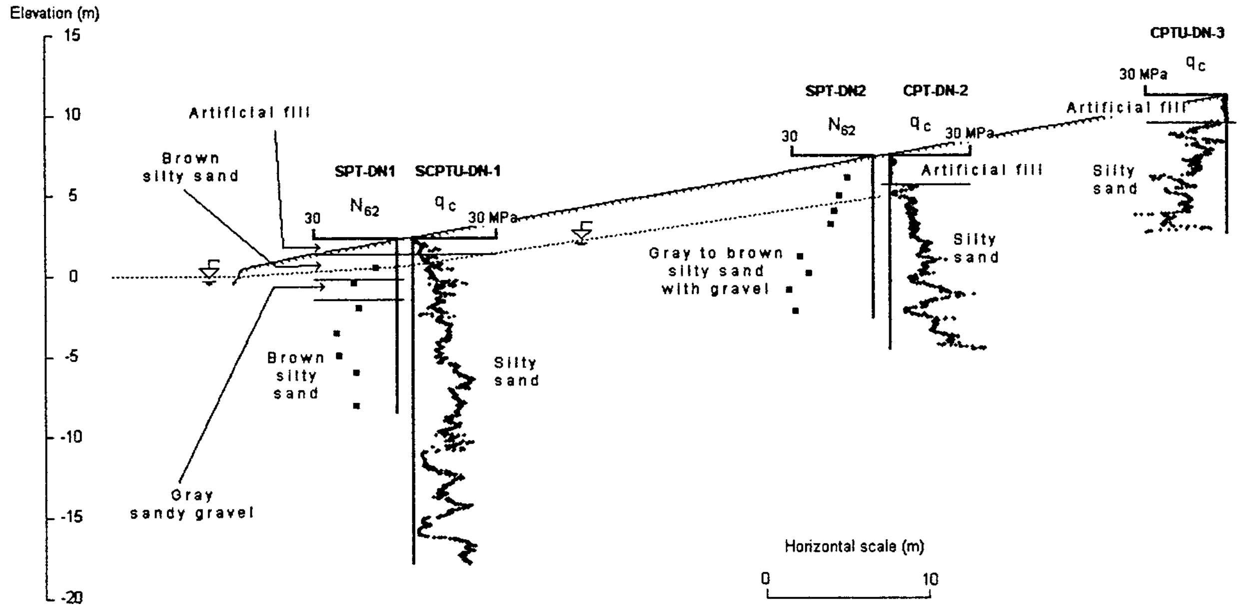

Fig. 11. Cross section I-I of Degirmendere Nose site

and reach a total of about 0.3 m at the shore of Izmit Bay along the cross section I in Fig. 13. Localized mapping of ground displacements was facilitated by ground surveys.

Evaluation of Liquefaction-Induced Lateral Ground Displacements

In this section, lateral ground displacement predictions based on the methodologies proposed by: (1) Hamada et al. (1986), (2) Youd et al. (2002), and (3) Shamoto et al. (1998) will be presented for the police station, soccer field, Degirmendere Nose, and Yalova Harbor sites. Predictions from these models will be compared with actual ground displacements mapped immediately following the Kocaeli earthquake. However, before then, a brief summary of these predictive methods will be presented next.

The methods of Hamada et al. (1986) and Youd et al. (2002) are empirical methods, based on regression analyses of large suites of previous lateral spreading case histories. Hamada et al. (1986) predict the amplitude of horizontal ground displacement

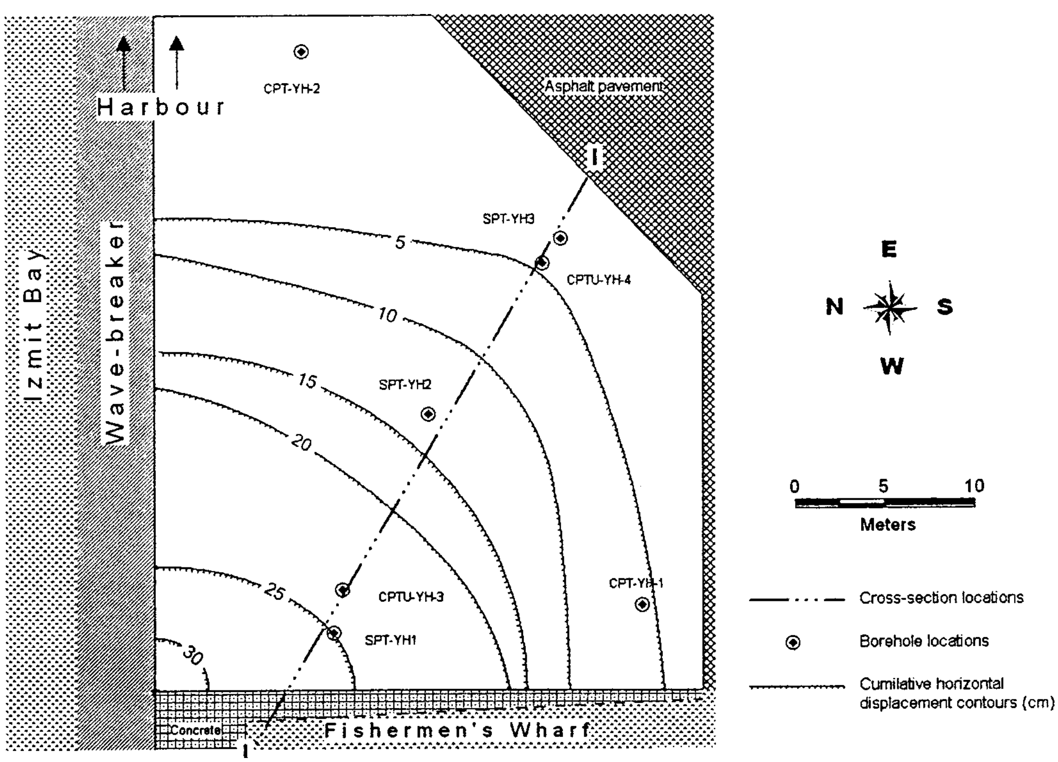

Fig. 12. Ground displacement map of Yalova Harbor site

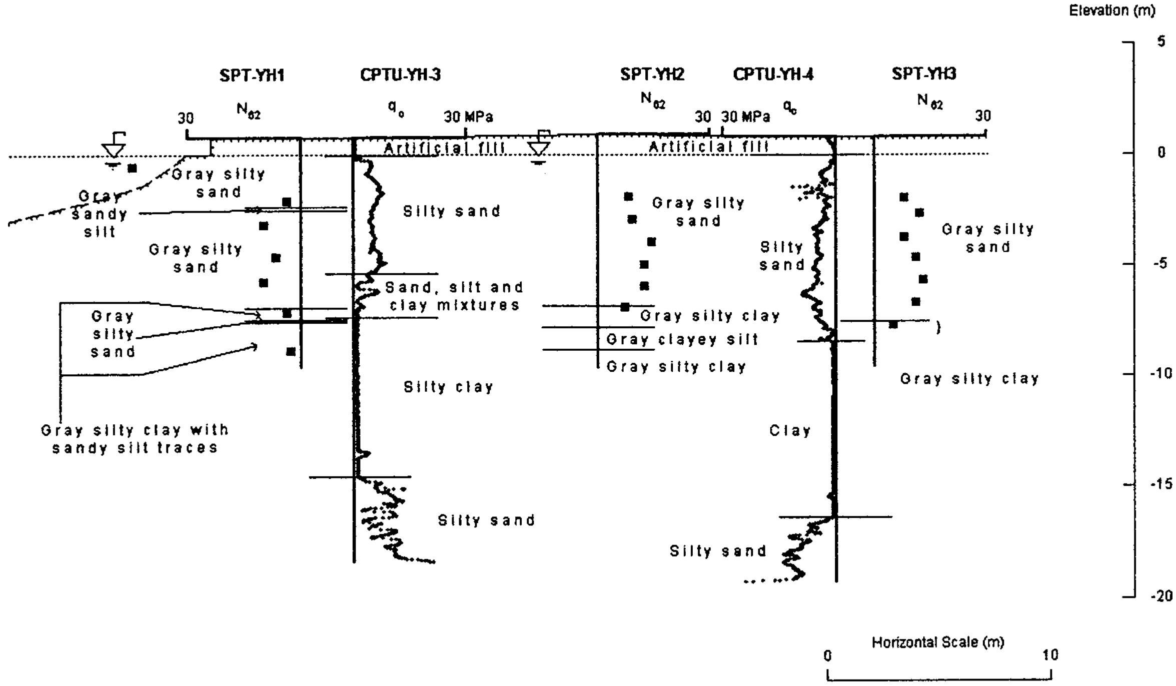

Fig. 13. Cross section I-I of Yalova Harbor site

from lateral spreading in terms of slope and thickness of the liquefied layers

$$D = 0.75 \times H^{0.75} \times \theta^{0.33} \tag{1}$$

where D=horizontal displacement (m); θ=slope (%) of the ground surface or the base of the liquefied soil; and H=total-thickness (m) of liquefied layers.

Bartlett and Youd (1992, 1995) introduced similar empirical models for predicting lateral spread displacements at liquefiable sites. The most recent version of the model (Youd et al. 2002) applies for either (1) sloping ground conditions or (2) relatively level ground conditions with a "free face" towards which lateral displacements may occur. The model was developed through multi-linear regression of a large case history database. Predictive models for the sloping ground and "free face" conditions are given in the following equations:

$$\begin{aligned}\log D_H = & -16.213 + 1.532M - 1.406 \log R^* - 0.012R \\ & + 0.338 \log S + 0.540 \log T_{15} + 3.413 \log(100 - F_{15}) \\ & - 0.795 \log(D50_{15} + 0.1\text{ mm})\end{aligned} \tag{2}$$

$$\begin{aligned}\log D_H = & -16.713 + 1.532M - 1.406 \log R^* - 0.012R \\ & + 0.592 \log W + 0.540 \log T_{15} + 3.413 \log(100 - F_{15}) \\ & - 0.795 \log(D50_{15} + 0.1\text{ mm})\end{aligned} \tag{3}$$

where D_H=horizontal ground displacement predicted by multiple linear regression model (m); M=earthquake magnitude (M_w was primarily used whenever reported); R=horizontal distance to nearest seismic source or to nearest fault rupture (km); $R^*=R+R_o$, and $R_o=10^{(0.89M-5.64)}$; S=gradient of surface topography or ground slope (%); W=free-face ratio, defined as the height of the free-face divided by its distance to calculation point; T_{15}=thickness of saturated layers with $(N_1)_{60} \leqslant 15$; F_{15}=average fines content (particles <0.075 mm) in T_{15} (%); and $D50_{15}$=average D_{50} in T_{15} (mm).

Shamoto et al. (1998) employed laboratory based estimates of the limiting shear strains in liquefied soil prior to the onset of dilation, coupled with an empirical adjustment factor to relate those limiting shear strains to observed field behavior, to estimate lateral spread displacements. This semiempirical method requires the determination of residual shear strain potential which was taken to be a function cyclic stress ratio (CSR), adjusted SPT N values, and fines content (FC). Fig. 14 presents the residual shear strain potential chart for clean sands. For the purpose of employing shear strain potential charts in Shamoto et al., in situ equivalent uniform cyclic shear stress ratios (CSR values) were estimated by employing "simplified procedures" (Seed and Idriss 1971) for PGA values of 0.3 g at the Yalova Harbor Site, and 0.4 g for the police station, soccer field, and Degirmendere Nose sites. Necessary corrections for earthquake duration, sloping ground, etc. were applied as part of the CSR estimation process. Adjusted N values are estimated simply as defined by Shamoto et al. (1998). Predicted residual shear strains are multiplied by the thickness of the liquefied layer to estimate potential residual lateral displacements across each liquefied layer. The summation of these residual lateral displacement values is then multiplied by an empirical factor of 1.0 or 0.16 in order to predict lateral displacements at the sites with or without "free face" ground conditions, respectively.

Using the above models, lateral ground displacements were estimated for a total of 4 sites and 10 borehole locations. Intermediate calculation steps of these analyses are presented in Tables 2–5, and the analysis results are summarized in Fig. 15 and Table 6 for comparison purposes. As shown by Fig. 15 and Table 6 for a significant number of lateral spread locations, predictions are off by a factor of more than 2 (i.e., predictions fall outside the region defined by 1:2 and 2:1 lines in Fig. 15). Predictions by the Youd et al. model are off by more than a factor of 2 for 5 out of 10 cases with the model generally overestimating the observed displacements. Similarly, 6 and 8 out of 10 lateral ground displacement predictions by Shamoto et al. and Hamada et al. models,

Table 2. Summary of Lateral Displacement Calculations for Police Station Site

Test: SPT-PS2								Observed horizontal displacement (cm): ∼240							
			Shamoto et al. (1998)					Hamada et al. (1986)		Youd et al. (2002)					
Depth (m)	SPT-N	USCS	N_a	Fines content (FC)	Cyclic stress ratio (CSR)	γ_r (%)	$(D_h)_{max}$ (cm)	H	θ	$(N_1)_{60}$	R	W	T_{15}	F_{15}	Remarks
2.1	8	SP-SM	15	12	0.36	18	18.0	3.7	10	14	0.5	8	2.7	12	
3.5	4	?	13	?	0.42	25	42.5			7	$(D_{50})_{15}$	M	Model		b
9.2	17	SW-SM	20	11	0.48	11	11.0			20	1.6	7.4	Free face		
Total displacement (cm):					72			310			300				
Test: SPT-PS3								**Observed horizontal displacement (cm): ∼10**							
			Shamoto et al. (1998)					Hamada et al. (1986)		Youd et al. (2002)					
Depth (m)	SPT-N	USCS	N_a	Fines content (FC)	Cyclic stress ratio (CSR)	γ_r (%)	$(D_h)_{max}$ (cm)	H	θ	$(N_1)_{60}$	R	W	T_{15}	F_{15}	Remarks
1.8	50+	SM	—	—	—	—	—	2.7	1	—	0.5	6	1.7	31	
2.7	3	SM	11	36	0.29	40	44.0			5	$(D_{50})_{15}$	M	Model		
8.5	6	SM	12	26	0.34	35	21.0			7					
11.8	38	SM	37	36	0.42	0	0.0			39	0.55	7.4	Free face		
Total displacement (cm):					$(65\times0.16=)10$			120			180				
Test: SPT-PS34								**Observed horizontal displacement (cm): ∼90**							
			Shamoto et al. (1998)					Hamada et al. (1986)		Youd et al. (2002)					
Depth (m)	SPT-N	USCS	N_a	Fines content (FC)	Cyclic stress ratio (CSR)	γ_r (%)	$(D_h)_{max}$ (cm)	H	θ	$(N_1)_{60}$	R	W	T_{15}	F_{15}	Remarks
1.6	8	GP-GM	14	11	0.27	18	22.0	1.7	1	12	0.5	8	1.2	11	a
7.8	16	SM	21	22	0.42	10	5.0			20	$(D_{50})_{15}$	M	Model		
											7.7	7.4	Free face		
Total displacement (cm):					$(27\times0.16=)4$			98			60				

[a]For settlement calculations of gravelly and silty deposits, procedures for sands are considered to be applicable.

[b]Fines content (FC) value is estimated due to lack of soil sample.

Table 3. Summary of Lateral Displacement Calculations for Soccer Field Site

Test: SPT-SF5								Observed horizontal displacement (cm): ∼30							
			Shamoto et al. (1998)					Hamada et al. (1986)		Youd et al. (2002)					
Depth (m)	SPT-N	USCS	N_a	Fines content (FC)	Cyclic stress ratio (CSR)	γ_r (%)	$(D_h)_{max}$ (cm)	H	θ	$(N_1)_{60}$	R	W	T_{15}	F_{15}	Remarks
2.1	4	SM	11	16	0.37	40	56.0	2.2	0	7	0.5	7	2.2	41	
3.1	3	ML	14	66	0.41	25	20.0			5	$(D_{50})_{15}$	M	Model		a
											1.3	7.4	Free face		
Total displacement (cm)					$(76\times0.16=)12$			0			74				
Test: SPT-SF6								**Observed horizontal displacement (cm): ∼120**							
			Shamoto et al. (1998)					Hamada et al. (1986)		Youd et al. (2002)					
Depth (m)	SPT-N	USCS	N_a	Fines content (FC)	Cyclic stress ratio (CSR)	γ_r (%)	$(D_h)_{max}$ (cm)	H	θ	$(N_1)_{60}$	R	W	T_{15}	F_{15}	Remarks
2.2	2	ML	12	52	0.39	35	49.0	1.4	0	3	0.5	15	1.4	52	a
											$(D_{50})_{15}$	M	Model		
											0.074	7.4	Free face		
Total displacement (cm):					49			0			240				

[a]For settlement calculations of qravelly and silty deposits, procedures for sands are considered to be applicable.

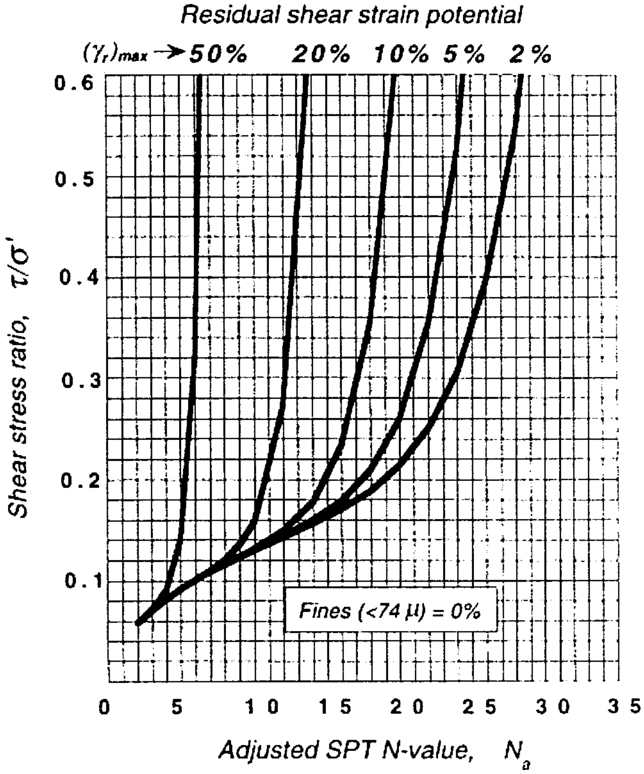

Fig. 14. Residual shear strain estimation charts for fines content (<74 μ) equal to (a) 0%, (b) 10%, and (c) 20%, respectively, after Shamoto et al. (1998)

respectively, are off by more than a factor of 2, with roughly comparable numbers of overpredictions and underpredictions. Several factors may contribute to these inconsistent predictions, and among all these, more common and general ones are as follows:

1. Our estimations of the predictive model parameters (e.g., thickness of the liquefied layer, representative SPT blowcounts, fines content in the critical stratum, peak ground acceleration, CSR, etc.) are prone to uncertainty due to limited available data and potential unknown spatial variations of properties.
2. The identification of potentially liquefiable layers as well as the contributions from those layers to the overall mapped residual lateral ground displacements, introduces uncertainties associated with epistemic variability in seismic soil liquefaction initiation methodologies.
3. Mapped lateral ground displacements could be in error due to mapping procedures used in the field, which generally involved summing displacements across ground fissures. Additional displacement associated with ground extension that is not manifest in fissures may have occurred, which would result in under-reporting of actual displacements. If so, displacements for these larger, undetected lateral spreads should be added to those measured at the site, which would increase the total spread displacements.
4. Estimated lateral ground displacements could be potentially on the low side due to unrepresented contributions from soft cohesive layers along the whole length of the characterized

Table 4. Summary of Lateral Displacement Calculations for Degirmendere Nose Site

Test: SPT-DN1								Observed horizontal displacement (cm): ~90							
			Shamoto et al. (1998)					Hamada et al. (1986)		Youd et al. (2002)					
Depth (m)	SPT-N	USCS	N_a	Fines content (FC)	Cyclic stress ratio (CSR)	γ_r (%)	$(D_h)_{max}$ (cm)	H	θ	$(N_1)_{60}$	R	W	T_{15}	F_{15gg}	Remarks
2.1	8	SM	16	20	0.30	20	16.0	5.4	17	14					
3.1	16	GW-GM	24	7	0.37	5	7.0			29	0.5	20	0.8	20	a
4.6	14	SM	24	40	0.40	7	8.4			21					
6.1	22	SM	27	14	0.43	3	4.8			29	$(D_{50})_{15}$	M	Model		
7.5	21	SW-SM	24	10	0.44	6	7.8			25					
8.6	15	SP-SM	17	9	0.45	16	16.0			17	2.9	7.4	Free face		
9.6	16	SW-SM	16	8	0.46	18	19.8			17					
10.6	15	SM	18	17	0.46	17	17.0			16					b
Total displacement (cm):					97			440				120			

Test: SPT-DN2								Observed horizontal displacement (cm): ~0							
			Shamoto et al. (1998)					Hamada et al. (1986)		Youd et al. (2002)					
Depth (m)	SPT-N	USCS	N_a	Fines conent FC	Cyclic stress ratio CSR	γ_r (%)	$(D_h)_{max}$ (cm)	H	θ	$(N_1)_{60}$	R	W	T_{15}	F_{15}	Remarks
2.7	13	SM	23	14	0.27	2	1.0	3	17	24					
3.7	15	SP-SM	23	11	0.32	4	4.0			24	0.5	5	0	—	
4.5	16	SM	23	13	0.35	5	7.5			24					
6.6	27	SW-SM	30	10	0.41	0	0.0			34	$(D_{50})_{15}$	M	Model		
7.6	24	SW-SM	23	6	0.43	6	7.2			30					
8.6	31	SM	33	17	0.44	0	0.0			36	—	7.4	Free face		
9.9	29	SW-SM	29	10	0.46	0	0.0			32					b
Total displacement (cm):					$(20\times0.16=)3$			440							0

[a]For settlement calculations of gravelly and silty deposits, procedures for sands are considerated to be applicable.

[b]Borehole ends in a sand layer: deeper send deposits may add additional displacements.

Table 5. Summary of Lateral Displacement Calculations for Yalova Harbor

Test: SPT-YH1								Observed horizontal displacement (cm): ~20							
			Shamoto et al. (1998)					Hamada et al. (1986)		Youd et al. (2002)					
Depth (m)	SPT-N	USCS	N_a	(FC)	Cyclic stress ratio (CSR)	γ_r (%)	$(D_h)_{\max}$ (cm)	H	θ	$(N_1)_{60}$	R	W	T_{15}	F_{15}	Remarks
1.6	45	SP-SM	56	11	0.33	0	0.0	6.5	0	68	35	20	4.2	19	
3.1	4	SP-SM	12	34	0.33	33	46.2			7					
4.2	10	SP-SM	21	46	0.34	8	9.6			16	$(D_{50})_{15}$	M	Model		
5.7	7	SP-SM	12	10	0.34	33	46.2			10	0.23	7.4	Free face		
6.8	10	SP-SM	15	14	0.34	18	25.2			13					
Total displacement (cm):					(127×0.16=)20			0			79				

Test: SPT-YH2								Observed horizontal displacement (cm): ~15							
			Shamoto et al. (1998)					Hamada et al. (1986)		Youd et al. (2002)					
Depth (m)	SPT-N	USCS	N_a	(FC)	(CSR)	γ_r (%)	$(D_h)_{\max}$ (cm)	H	θ	$(N_1)_{60}$	R	W	T_{15}	F_{15}	Remarks
3.1	8	?	16	?	0.34	18	45.0	7.9	0	13	35	13	3.6	20	[a]
4.1	9	SM	18	26	0.34	14	15.4			15					
5.1	14	?	21	?	0.34	8	12.8			21	$(D_{50})_{15}$	M	Model		[a]
6.2	12	SM	18	17	0.34	14	21.0			16	0.21	7.4	Free face		
7.1	12	SM	18	26	0.34	14	16.8			16					
Total displacement (cm):					(111×0.16=)18			0			57				

Test: SPT-YH3								Observed horizontal displacement (cm): ~5							
			Shamoto et al. (1998)					Hamada et al. (1986)		Youd et al. (2002)					
Depth (m)	SPT-N	USCS	N_a	(FC)	(CSR)	γ_r (%)	$(D_h)_{\max}$ (cm)	H	θ	$(N_1)_{60}$	R	W	T_{15}	F_{15}	Remarks
3.0	8	SM	16	16	0.33	18	43.2	7.5	0	13					
3.7	12	SP-SM	20	11	0.33	8	6.4			20	35	8	5.7	18	
4.8	8	SP-SM	14	10	0.34	20	20.0			12					
5.7	11	SM	16	11	0.34	16	16.0			15	$(D_{50})_{15}$	M	Model		
6.7	13	SM	18	17	0.34	14	14.0			17	0.20	7.4	Free face		
7.7	11	SM	15	33	0.34	20	26.0			14					
Total displacement (cm):					(126×0.16=)20			0							61

[a]Fines content (FC) value is estimated due to lack of soil sample.

soil profiles and from cohesionless soil layers below maximum depth of site characterization.

5. Free face or sloping ground models were employed for the estimation of lateral displacements. However some sites may be better represented by a combination of sloping ground and free face, for which empirical models are not available.

Additional factors that may partially explain the biased predictions for specific models are provided below:

1. Near-field peak ground accelerations recorded in the Kocaeli earthquake were generally smaller than those predicted by standard attenuation relationships, indicating that ground shaking may not have been as intense at these sites as the average for sites (in previous earthquakes) used in the development of the predictive empirical relationships. Thus, the actual motions at the site would have been less intense than those implicit in Youd et al. (2002) empirical predictions, which would be expected to result in overprediction of lateral displacements.
2. The Youd et al. (2002) predictions are sensitive to the values adopted for free face ratio, which were estimated from available bathymetry maps and/or site observations. Inconsistent predictions at the Degirmendere site might be due in part to inaccurate estimation of free face ratio values as they existed prior to the earthquake.
3. The Hamada et al. (1986) predictions are very sensitive to the value adopted for the ground slope, and poor predictions might be simply due to inaccurate estimation of "average" ground slope values.
4. The underprediction from the Shamoto et al. (1998) method may have been due in part to the fact that the recommended correction factor of 0.16 for a sloping site becomes a major factor in the reliability of estimations. Using just this single factor, the Shamoto et al. (1998) procedure does not account well for variable "driving" static shear stresses arising from edge slope geometries.

Due to either uncertainty in input parameters and/or shortcomings of the models, the three state-of-practice predictive methodologies considered herein do not produce lateral ground displacement predictions with acceptable engineering accuracy. Thus, it appears that there is a need for improved engineering tools for prediction of small to moderately significant lateral spread ground displacements (~0.1–2.5 m) at soil sites with similar ground characteristics to the case history sites presented herein.

Summary and Conclusions

Liquefaction-induced lateral ground displacements at five soil sites strongly shaken by the 1999 Kocaeli-Turkey earthquake

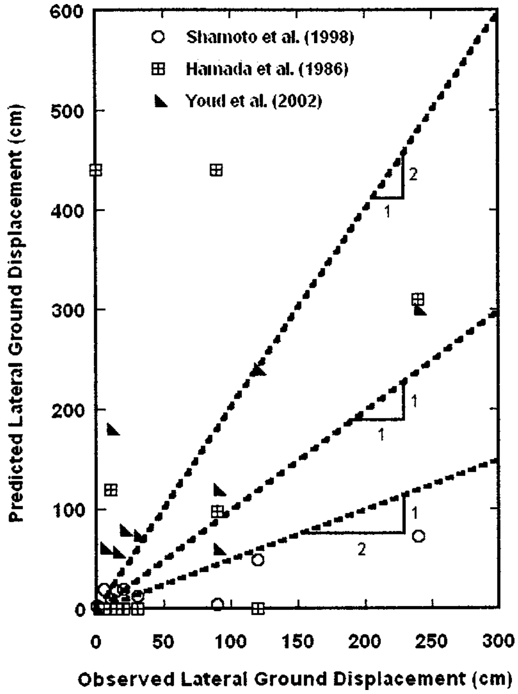

Fig. 15. Comparison of predicted versus observed lateral spreading displacements

have been documented and studied. Field measurements of ground displacements were generally performed within 1–3 weeks following the earthquake. For the purpose of subsurface characterization, wash rotary borings with SPT, CPT, and CPTU soundings were performed. Results of subsurface characterization studies were used to "predict" lateral displacements, using the methodologies proposed by Hamada et al. (1986), Shamoto et al. (1998), and Youd et al. (2002).

The empirical method of Youd et al. (2002) tended to overpredict the observed lateral ground displacements. In addition to the uncertainties in the estimation of predictive model parameters (e.g., thickness of the liquefied layer, representative SPT blowcounts, peak ground acceleration, CSR, etc.), this was likely due, in large part, to the inaccuracies in classifying the site either as a free face or a sloping ground site. An additional factor was the levels of shaking at the sites, which were less severe than would have been predicted by most contemporary attenuation relationships, and so were somewhat less severe than the levels of shaking implicit in these empirical lateral displacement prediction methodologies. The methodologies of Hamada et al. (1986) and Shamoto et al. (1998) tended to either underpredict or overpredict the observed lateral ground displacements by large amounts. However, the Shamoto et al. procedure requires a large correction factor (multiplication by 0.16) to correlate laboratory-based limiting shear strains with expected field values. This factor is based, in part, on definition of the site as "sloping, but without a free face." As the sites, in fact, might have been better characterized as having ground slope and free faces, this correction may warrant adjustment.

Overall, as shown in Fig. 14 and summarized in Table 6, these state-of-practice analytical tools provide relatively inconsistent predictions of observed lateral ground displacements. Thus, it appears that there is a need for improved engineering tools for the prediction of small to moderate lateral ground displacements (~0.1–2.5 m.) at soil sites with similar ground characteristics to the case history sites presented herein.

Table 6. Comparison of Predicted versus Observed Lateral Spreading Displacements

		Lateral ground spread (cm)			
Site	Borehole number	Observed	Shamoto et al. (1998)	Hamada et al. (1986)	Youd et al. (2002)
Police station	PS2	240	72	310	300
	PS3	10	10	120	180
	PS4	90	4	98	60
Soccer field	SF5	30	12	0	74
	SF6	120	49	0	240
Degirmendere nose	DN1	90	97	440	120
	DN2	0	3	440	0
Yalova harbor	YH1	20	20	0	79
	YH2	15	18	0	57
	YH3	5	20	0	61

Acknowledgments

These studies were funded by the U.S. National Science Foundation under Grant Nos. CMS-9987829 and CMS-0085130, and by the California Department of Transportation (CALTRANS), the California Energy Commission (CEC), and Pacific Gas and Electric Company (PG&E) through the Pacific Earthquake Engineering Research Center's Lifelines Program under Award No. 3A01. In-kind support was provided by Zetas Corporation through the field CPT and drilling efforts. All of this support is gratefully acknowledged.

References

Abrahamson, N. A., and Silva, W. J. (1997). "Empirical response spectral attenuation relations for shallow crustal earthquakes." *Seismol. Res. Lett.*, 68(1), 94–127

American Society for Testing and Materials (ASTM). (2000). "Standard practice for determining the normalized penetration resistance of sands for evaluation of liquefaction potential." *D 6066-96*, West Conshohohocken, Pa.

Bartlett, S. F., and Youd, T. L. (1992). "Empirical analysis of horizontal ground displacement generated by liquefaction-induced lateral spreads." *Tech. Rep. No. NCEER-92-0021*, National Center for Earthquake Engineering Research, State Univ of New York at Buffalo, Buffalo, N.Y.

Bartlett, S. F., and Youd, T. L. (1995). "Empirical predictions of liquefaction-induced lateral spread." *J. Geotech. Eng.*, 121(4), 316–329.

Cetin, K. O., Isik, N., and Unutmaz, B. (2004). "Seismically-induced landslide at Degirmendere Nose, Izmit Bay after 1999 Kocaeli (Izmit)—Turkey Earthquake." *Soil Dyn. Earthquake Eng.*, 24(3), 189–197.

Goncuoglu, M. C., Erendil, M., Tekeli, O., Aksay, A., Kuscu, I., and Urgun, B. M. (1992). "Introduction to the geology of Armutlu Peninsula." *Proc. Int. Symp. on the Geology of the Black Sea Region*, MTA, Ankara, Turkey, 26–32.

Hamada, M., Yasuda, S., Isoyama, R., and Emoto, K. (1986). "Study on liquefaction-induced permanent ground displacements." Association for the Development of Earthquake Prediction, Japan.

Idriss, I. M., and Sun, J. I. (1992). *SHAKE91: A computer program for conducting equivalent linear seismic response analyses of horizontally layered soil deposits*, Center for Geotechnical Modeling, Univ. of California, Davis, Calif.

Safak, E. et al., "Recorded main shock and aftershock motions." *Earthquake Spectra*, 16(16), 97–112.

Seed, H. B., and Idriss, I. M. (1971). "Simplified procedure for evaluating soil liquefaction potential." *J. Soil Mech. Found. Div.*, 97(9), 1249–1273.

Seed, H. B., Tokimatsu, K., Harder, L. F., and Chung, R. M. (1985). "The Influence of SPT procedures in soil liquefaction resistance evaluations." *J. Geotech. Eng.*, 111(12), 1425–1445.

Seymen, I. (1995). "Geology of the Izmit Gulf Region (NW Turkey)." *Quaternary sequence in the Gulf of Izmit*, I. Meric, ed., ISBN 975-96123-0-5.

Shamoto, Y., Zhang, J., and Tokimatsu, K. (1998). "New charts for predicting large residual post-liquefaction ground deformations." *Soil dynamics and earthquake engineering*, Vol. 17, Elsevier, New York, 427–438.

Youd, T. L., Hansen, C. M., and Bartlett, S. F. (2002). "Revised multilinear regression equations for prediction of lateral spread displacement." *J. Geotech. Geoenviron. Eng.*, 128(12), 1007–1017.